Influence of white etching bands formation on integrity of rolling element bearings

Mostafa El Laithy[a], Ling Wang[a], Terry J. Harvey[a], Bernd Vierneusel[b]

[a]*National Center for Advanced Tribology at Southampton (nCATS), University of Southampton, University Road, Southampton SO17 1BJ, UK*

[b]*Schaeffler Technologies AG & Co. KG, Georg-Schäfer-Straße 30, 97421 Schweinfurt, Germany*

Abstract

The development of subsurface microstructural alterations known as dark etching regions (DERs) and white etching bands (WEBs) in rolling element bearings due to rolling contact fatigue have been investigated for the past eight decades, focusing on their initiation and formation mechanisms. They have only recently been shown to be driven by repetitive cycles of energy build-up due to micro-plastic deformation and energy release through recrystallization and recovery, which results in the formation of equiaxed and elongated ferrite grains, as well as lenticular carbides. These features develop within the bearing subsurface from DER to WEBs during bearing operation at moderate to high loads, but little evidence has been presented in the literature to understand links between DER and WEBs and the nucleation and growth of subsurface cracks. This investigation examines WEBs, including low angle bands (LABs) and high angle bands (HABs), in detail especially focusing on their late stages to understand such links. A number of techniques, including optical microscopy, scanning electron microscopy (SEM) and Energy-dispersive X-ray spectroscopy (EDX) have been used to examine the features involved. Analysis on WEBs obtained through serial sectioning has revealed that voids initiating at the interface between lenticular carbides and equiaxed ferrite grain bands within WEBs have led to crack formation which can subsequently propagate to bearing surfaces. Interactions between WEBs and non-metallic inclusions (NMIs) are observed to lead to de-bonding of inclusions from their surrounding microstructure and void formation, which has also found to influence the integrity of the bearings at late stages. Alumina and Manganese sulphide (MnS) inclusions are the mostly observed NMIs that de-bond and develop microcracks when interacting with WEBs. These findings thus provide important insights into the link between inclusions and crack initiation and represent a further step towards a fundamental understanding of the rolling contact fatigue process.

1. Introduction

The study of rolling contact fatigue (RCF) induced subsurface microstructure alterations in bearing steels has been investigated for decades [1, 2, 3], amongst which 'white etching matters' has been a common feature in several microstructural alterations including white etching layer (WEL) [4], white etching crack (WEC) , butterflies and white etching bands (WEBs) [1, 3, 5, 6]. Of the features, WECs and butterflies are 'localized' microstructural alterations. While WEBs are 'global' microstructural alterations that form and develop in the highest stressed regions [1].

A particular interest in studying WECs, which are cracks bordered by white etching area (WEA), has been developed from its correlation with early bearing failure in various industries such as wind turbine gearboxes, occurring within 10% of their L_{10} life [3]. The formation mechanism of WECs is still not fully confirmed with the main debate on the order of crack and WEA formation [3, 7, 8, 9]. WEBs and butterflies however are associated with bearing operation at high number of revolutions i.e., toward, or even beyond their L_{10} life [1]. Butterfly formation, which can cause bearing failure, is generally considered to be caused by the elastic modulus differences, differing coefficient of thermal expansion (CTE) and the weak interfacial energy between the inclusion and the matrix generating tensile and shear stresses in the surrounding matrix [10, 11, 12]. This results in deformation and crack initiation/propagation in a direction comparable to the unidirectional shear stress, which may be influential in butterfly formation [13, 14, 15]. To the best knowledge of the authors, only two papers have evidenced cracks interacting with WEBs, by Maharjan et al. [16] and Martin et al. [17]. Martin et al. [17] partially cut a bearing inner ring that was previously RCF tested at an axial plane and fractured so that the cracking would proceed from the rolling surface down toward the bore on an axial plane. While this examination consisted on artificially induced crack in the bearing inner ring, by Maharjan et al. [16] reported cracks developing naturally within the bearing inner ring during RCF but it was not clear whether the cracks reached the bearing surface or lead to final bearing failure. Both studies had aimed at proposing a correlation between WEB formation and crack orientation patterns but had not focused on crack initiation sites, propagation and how such mechanisms impact microstructural integrity that might lead to final bearing failure.

WEBs typically appear at high numbers of revolutions and their formation is heavily dependent on material heat treatment and bearing operating conditions such as contact pressure, operating temperature and running time [1, 18, 19, 20]. They form within the maximum stress region due to formation of dark etching bands and refinement of the overall microstructure leading to stress point accumulation causing recrystallization [21]. They firstly develop in the form of low angle bands (LABs) typically from 100 million cycles, and are orientated approximately 30° to the rolling direction [22, 23]. As the density of LABs increases, high angle bands (HABs)

develop from 500 million cycles and are orientated at approximately 80° to the rolling direction [23]. LABs and HABs consist of similar features with HABs being typically larger in dimensions than LABs [20, 22]. Also, HABs are found to initially form within LABs as recrystallized equiaxed ferrite grain due to energy build-up accumulation in the region, followed by a recovery mechanism in the form of grain rotation/coalescence leading to the formation elongated ferrite grains which releases carbon initially segregated at grain boundaries to nucleate as lenticular carbides [24]. The equiaxed and elongated ferrite grains in WEBs (both LABs and HABs) are 30% and 38% softer than the parent martensitic microstructure respectively while the lenticular carbides are 37% harder than the steel matrix [24]. Many studies have been conducted on the formation mechanism of WEBs [24, 25, 17, 19] however no results have shown direct links between WEBs and bearing integrity, i.e. whether and how WEBs contribute to bearing failures.

One of the key parameters that influences bearing material integrity is steel cleanliness, which has been significantly improved over the years with much fewer and smaller inclusions in high quality bearing steels [26, 27] . However, inclusions cannot be completely removed, hence there is a need to better understand their influence of bearing integrity in detail. The steel examined in this study meets the high demands of the current bearing industry. Oxide inclusions such as alumina are found to be more detrimental to bearing life than other types due to their high brittleness and high hardness (about 2,200 HV) [28, 29]. Studies have shown that oxide inclusions could break up and lead to debonding from their surrounding matrix and under cyclic stresses hence, forming cavities that may cause fatigue spall in bearings [1, 28] . Modern bearing steel manufacturers aim to minimize the presence of such inclusions during manufacturing stage to below 10 ppm [27]. Sulphide inclusions in bearing steels are found to be softer than parent microstructure, for example MnS inclusions have a hardness ranging between 150-170 HV, and typically appear to be elongated in shape [1]. This is because, under stress induced deformation, MnS inclusions elongate, i.e. stretch out following the stress/strain orientations, in contrast to hard oxide inclusions [28, 30]. Oxides and sulphides have both been linked to the formation of butterflies but not directly through WEBs so far [3].

The aim of this study is to investigate the influence of WEBs on bearing integrity through the analysis of late-stage LABs and HABs formed in bearing samples with and without surface spall. Interactions between WEBs and inclusions have also been examined.

2. Methodology

The investigation has been carried out on a number of 7205 angular contact ball bearings (ACBBs), made from 100Cr6 martensitic bearing steel that were through hardened to 830 HV with S0-stabilization (industrial standard heat treatment set by controlling annealing temperatures to achieve operational stability at operating temperatures < 150 °C). The bearings have been RCF tested on the L-17 test rig at Schaeffler Technologies (detailed in [30]) at an operating temperature of 80°C lubricated by commercial gear oil (ISO VG 68) resulting in a viscosity ratio κ of 2.69 (ratio of operating viscosity to reference viscosity) under two contact pressures (2.9 and 3.5 GPa) over a range of stress cycles. The viscosity ratio is used in industry to assess the quality of lubrication film formation, where a value greater than 2 suggests a fully developed lubricant film [31]. Details of the test conditions and the samples being analysed in this study are given in Table 1, including five suspended bearings (bearings run for pre-determined number of cycles without any failure) and one failed bearing with surface spall damages detected at the inner ring.

Table 1 A summary of the bearing samples and their test conditions.

Stress Cycles	Contact Pressure (GPa)	Failure
4141×10^6	2.9	None
3016×10^6		
2341×10^6		
1448×10^6		
1116×10^6		
885×10^6	3.5	Surface Spall

All bearing samples have been examined using standard metallography preparation and microstructural analysis, including mechanical polishing of cut samples using 6 ,3 ,1 and 0.25 μm diamond suspensions, etched with 2% Nital before been examined optically using an Olympus BX51 light optical microscope (LOM) and scanning electron microscopy (SEM) by a JEOL JSM-6500F with an accelerating voltage of 15 kV. Energy dispersive X ray spectroscopy (EDX) has been conducted on regions of interest using an Oxford Inca 300 for elemental analysis embedded in the SEM to investigate inclusion composition.

3. Results

All samples in this study have WEBs developed within the microstructure (including LAB and HAB). As previously reported [23, 24], different developing stages of the WEBs have been observed cross the bearing samples tested from 1116 million - 4141 million cycles. This study will seek potential microstructural damages (voids and cracks) around WEBs.

3.1 WEBs in Suspended Bearing Samples

Figure 1 shows the various stage of microstructural alterations from early stage LABs, shown in Figure 1a), through densification of LAB regions, shown in Figure 1b), to HAB formation, shown in Figure 1c). These images were captured from three samples without any damages (e.g. voids or cracks) detected between the WEBs which consists of lenticular carbides and ferrite regions (pointed by black and white arrows respectively in Figure 1). Details of the WEB stages have been previously discussed in [24] by the authors of this paper.

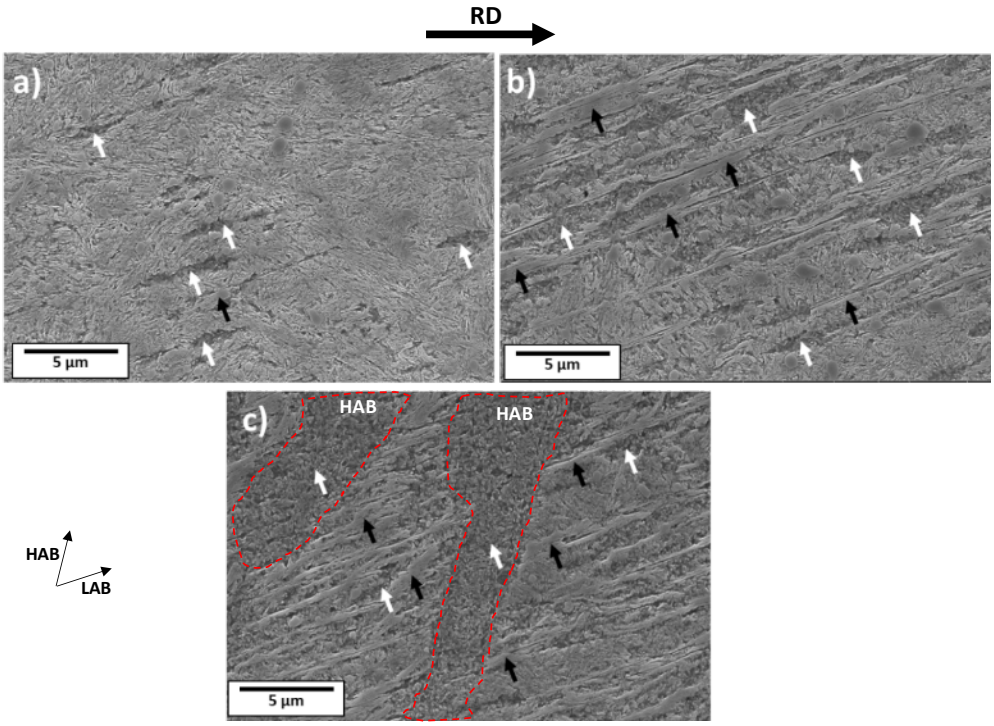

Figure 1: SEM images showing LABs and HABs without damages a) Early stage LABs (1116 million cycles). b) Late stage development of LAB (3016 million cycles). c) HABs formed from fully developed LABs) (4141 million cycles). Black and white arrows point to lenticular carbides and equiaxed ferrite regions respectively. Region highlighted in red corresponds to HABs.

While the majority of WEBs develop without any damages (i.e. cracks or voids) as shown in Figure 1, voids or micro-cracks have however been observed across LABs in several samples, see examples given in Figure 2 and Figure 3 in late-stage LABs from samples run for 4141 and 3016 million cycles respectively. Both bearings have developed voids/micro-cracks parallel to LABs between the lenticular carbide and ferrite interface as shown by the black and white arrows respectively. The micro-cracks observed are of 1 to > 10 µm in length and < 2 µm in width.

A question arose during this study on the nature of these voids/cracks observed in LABs and whether they were a product of surface preparation and etching or real artifacts developed from the RCF-induced microstructural

transformation in the form of LABs, further detailed analysis of has been conducted through manual serial sectioning of these features in a late-stage sample run for 4141 million cycles (see Figure 4). Twelve slices were captured at 1 µm intervals, giving a total removal thickness of 12 µm. The shown continuity of the crack through the whole 12 µm thickness as well as the crack getting smaller from slice 1 to 12 suggests it is unlikely an artifact of etching or polishing. It is interesting to note that the crack appears to be surrounded by the lenticular carbides (yellow arrows) which becomes more obvious as the crack reduces from Figure 4 (slices 3-8). It can also be seen from Figure 4 (slices 9-12) that as the crack reduces, a clear interface between the lenticular carbides and ferrite regions (red arrows) exists in the location where voids used to be. This provides strong evidence of these cracks originating at the interface of the ferrite region and lenticular carbides which is proposed to be a plane of weakness in the LABs. It is proposed that these cracks develop at these sites as a consequence of mechanical loading on weak planes between the ferrite-lenticular carbide or a consequence of potential volume change associated with the microstructural transformation of martensite to ferrite, which is linked to a reduction in volume. Hence stress point accumulation at these weak planes could reach a critical point when a high density of the LAB has developed, leading to void/crack formation across the microstructure. More evidence of these micro-cracks in etched and unetched samples is explored later in more detail in section 3.2.

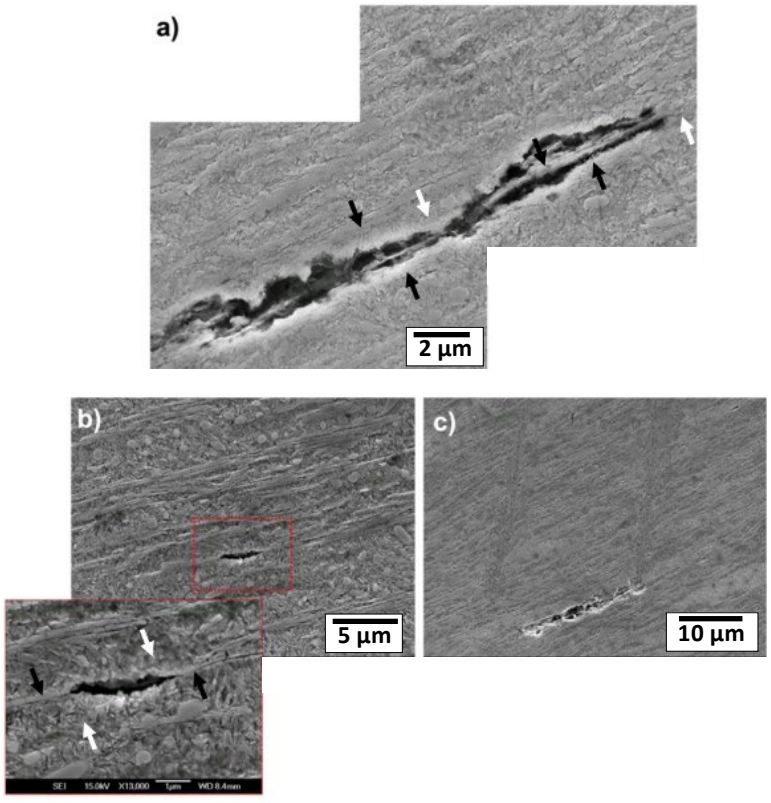

Figure 2: SEM images showing various cracks observed across LAB features in a bearing sample run for 4141 million cycles. Black and white arrows indicate lenticular carbides and equiaxed ferrite grains respectively.

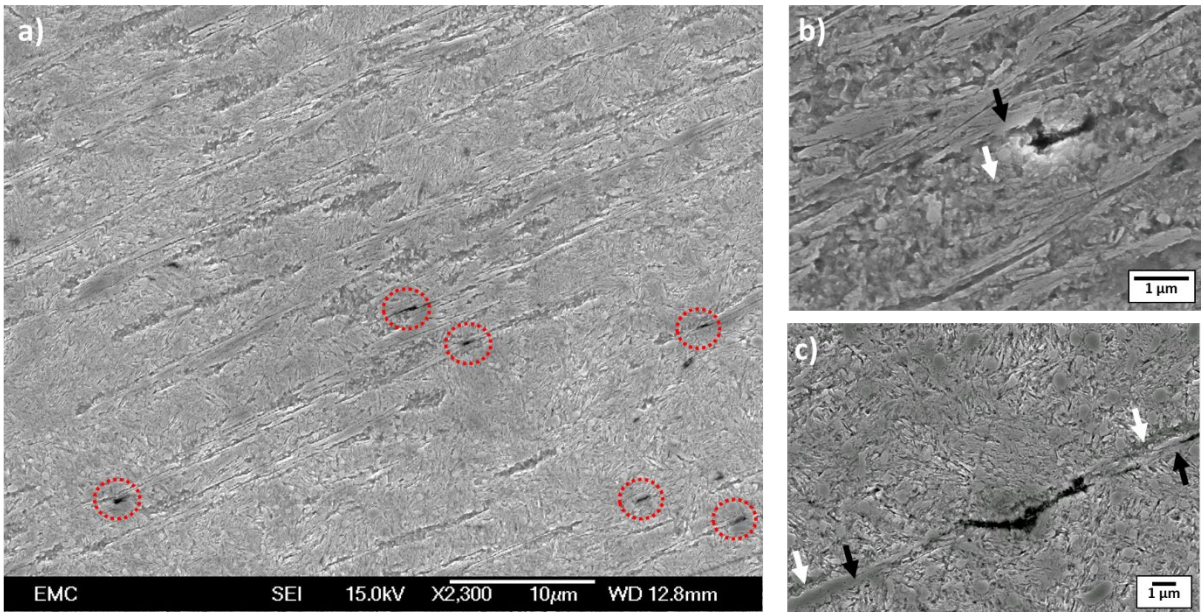

Figure 3: SEM images showing voids/cracks across LABs in the sample tested for 3016 million cycles a) multiple sub-micron voids formed across LABs (indicated by red circles); b) A zoom-in image showing one of the small voids at ~1 µm length .c) a larger void/crack of a few µm length. Black and white arrows indicate lenticular carbides and equiaxed ferrite grains respectively.

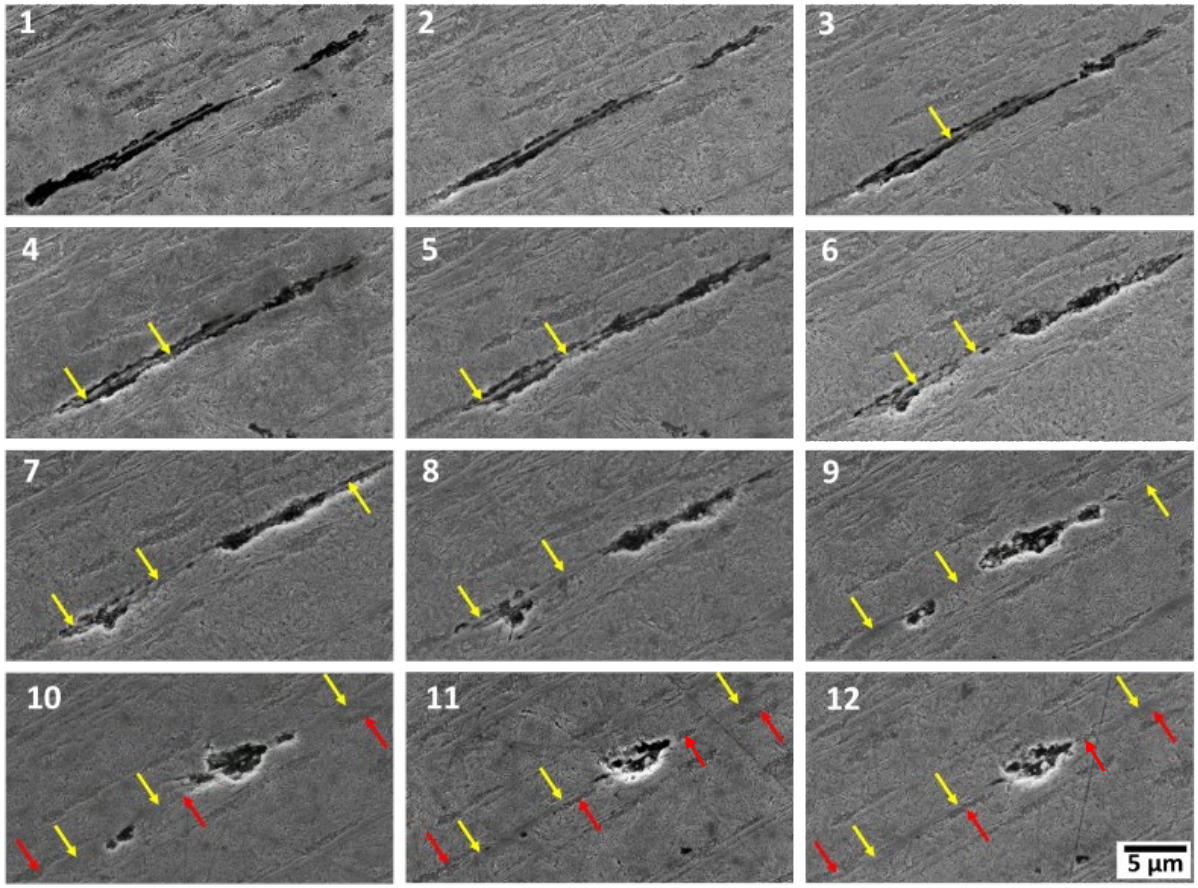

Figure 4: SEM images from a serial sectioning of a crack feature observed in LABs in a sample from the 4141 million cycles bearing, showing 12 consecutive sections at 1 µm intervals. Yellow arrows show the lenticular carbides while red arrows show equiaxed ferrite regions.

The formation of these cracks at the interface of the lenticular carbide/ferrite is strong evidence that these weak

planes can impact the integrity of the microstructure during RCF as the LABs develop. These voids/cracks have been observed in both dense and sparse regions of LAB as shown in Figure 5 (details on dense and spare WEBs is discussed in [22]). However, they are more frequent in the regions with dense LABs compared to spare regions. This coupled with that earliest stage bearing test in this study (run for 1116 million cycles) presenting no voids across LABs confirms these subsurface cracks are a consequence of LAB formation and densification rather than metallographic preparation where stress point accumulation at these weak planes could reach a critical point when dense LAB regions/areas develop. As evidenced from Figures 2-5, these voids/cracks are observed to the LABs rather than HABs. This could be linked to the formation mechanism reported in [24] where the LABs are associated with a build-up of energy in the microstructure stemming from the unstable geometry of the carbides while the HAB is a form of energy release.

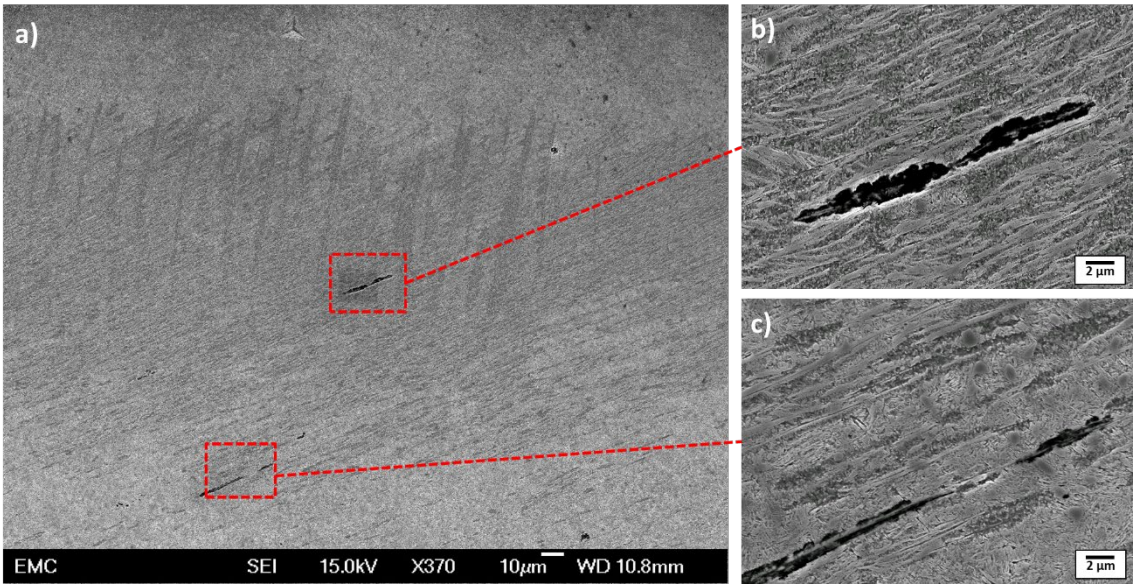

Figure 5: Voids formed in WEB regions in a sample from the 4141 million cycles bearing with zoom-in images b) in a dense region and c) in a region of sparse LABs.

3.2 Non-metallic Inclusions (NMIs) interaction with WEBs in suspended samples

The previous section discussed voids and micro-cracks developing across weak planes of the LABs that lead to bearing damages however the role of NMIs in steels on bearing integrity is also often questioned. It is well known that steel cleanliness is a significant factor in bearing life. In this section, interactions between WEBs and inclusions are investigated. Figure 6 shows a number of SEM images of NMIs observed in the bearing samples tested for a variety of stress cycles captured at a depth of 60-250 µm, which is the region in the subsurface where WEBs are found to be fully developed [22, 23, 24]. This is to determine whether the interaction between WEBs and NMIs can initiate or accelerate crack formation. Figure 6a shows an alumina inclusion fully embedded

between a LAB and HAB with micro-cracks observed within the inclusion at orientations similar to LAB and HAB. A similar observation is recorded in Figure 6c for an MnS inclusion, where a small crack is seen to stem from the edge of the inclusion and a LAB penetrates. This indicates that micro-cracks develop within inclusions when they are penetrated by WEBs. All inclusions have shown to have de-bonded from the surrounding microstructure (forming cavities between inclusion/matrix), which are potential failure initiation sites in bearings and have been more commonly observed in inclusions surrounded by WEB compared to inclusions surrounded by the parent matrix. Therefore, they are potential failure sites in the bearing microstructure as the coherence of inclusions with surrounding microstructure is compromised. On the other hand, inclusions positioned away from WEBs have not shown such cracks or cavities as presented in Figure 7, which was captured from the late stage bearing sample run for 4141 million cycles. For both duplex (consisting of alumina and MnS) and pure MnS inclusions in Figure 7a and Figure 7b respectively, good coherence with the surrounding microstructure is preserved. It should be noted that inclusions observed in this study have a diameter < 10 µm, which are smaller than those typically investigated reported in other features such as butterflies [3, 32].

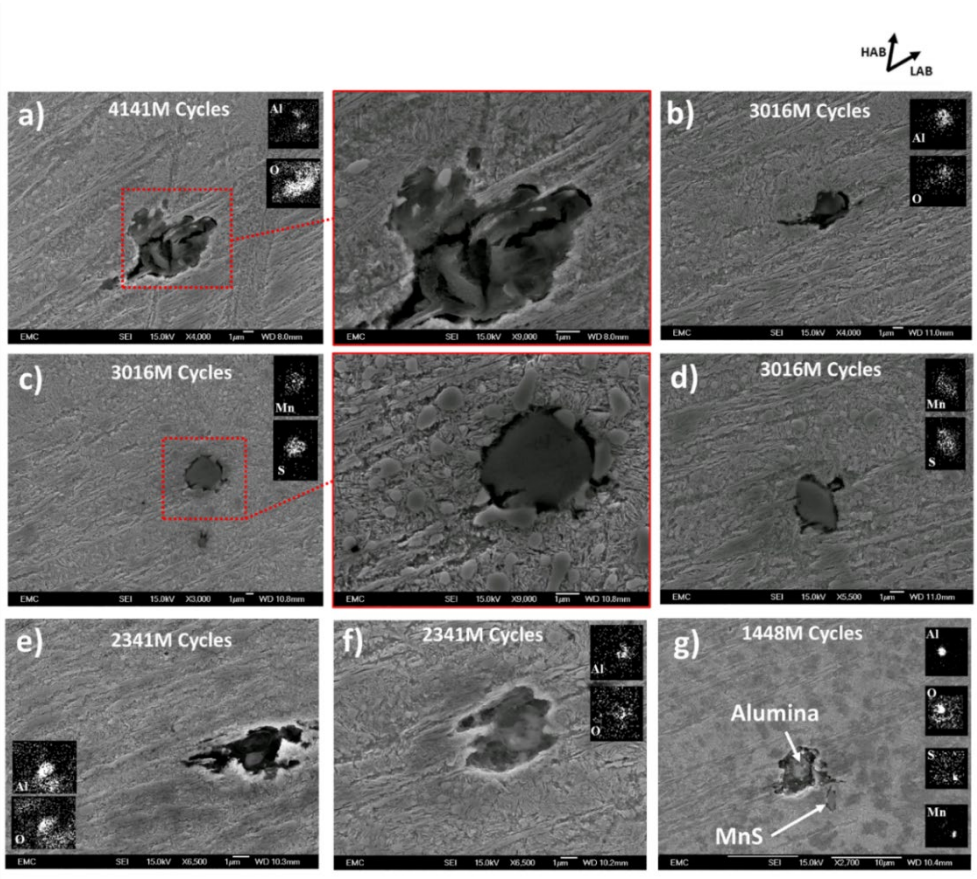

Figure 6: SEM and EDX elemental maps of different inclusions located within the vicinity of WEB from different samples run for different stress cycles. a,c) Shows microcracks developing within the inclusions at orientations similar to surrounding LAB and HAB. b,d-g) shows loss of coherence between the inclusion/microstructure interface when surrounded by LAB. Inclusions a,b,e,f are Alumina while c,d are MnS inclusions. g) shows seperate MnS and Alumina inclusions in close proximity.

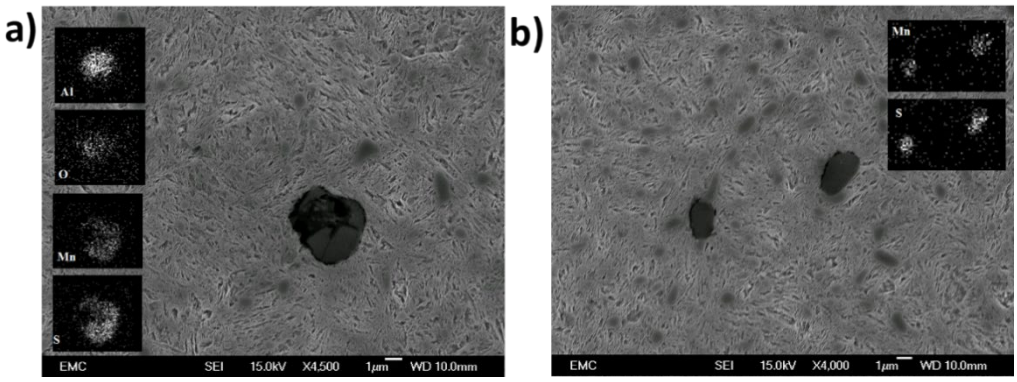

Figure 7: SEM and EDX map of inclusions developing away from the WEB region showing a) Duplex inclusion from sample run for 2341 million cycles and b) MnS inclusions from sample run for 3016 million cycles.

De-bonding of inclusions from the WEB affected surrounding microstructure is also found to lead to easily removal of the inclusions during metallographic preparation (see examples shown in Figure 8). This loss of coherence and cavity formation may be linked to the reduction in lattice volume during the transformation of martensite to ferrite [33, 34]. As the cavities develop around inclusions embedded within the LABs, Figure 8 suggests cracks propagate from the interface of the surrounding matrix/inclusion to the weak planes across the LABs (lenticular carbide/ferrite interface). The crack formations at the edge of inclusions (see examples shown in Figure 8a,c) resemble that associated with butterflies. However, no microstructural transformation is observed along the crack other than LABs. The cracks at the edge of the inclusions in Figure 8a,c also resemble the voids/cracks observed across LABs shown in Figure 2-4.

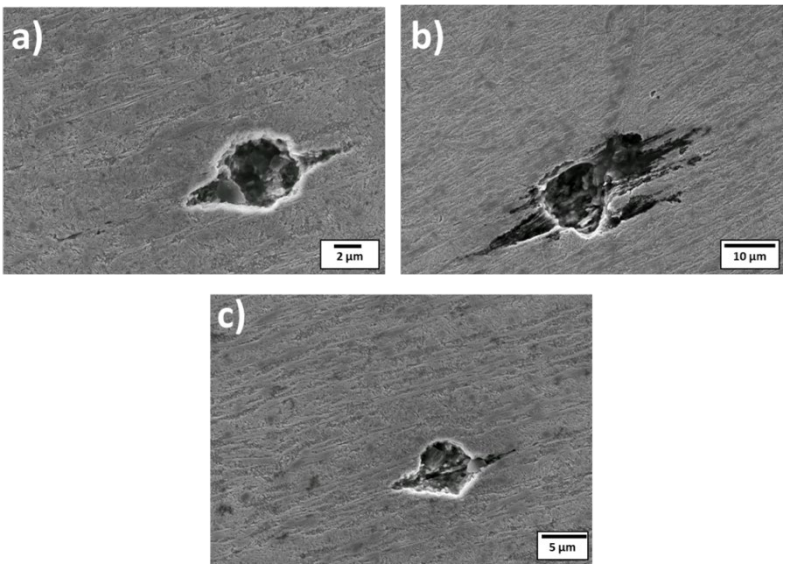

Figure 8: SEM images of cracks in the etched surface of samples where inclusions embedded within WEBs have been removed due to crack formation parallel to LAB and loss of coherency with surrounding microstructure. Images a) and c) where captured from bearing sample run for 2341 million cycles and b) was captured from sample run for 4141 million cycles.

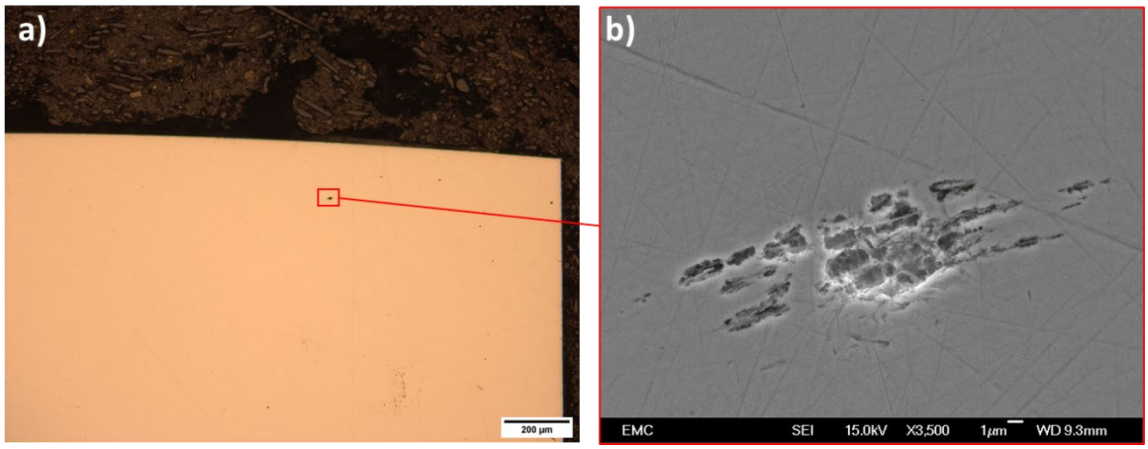

Figure 9: a) An optical image of unetched surface from a sample of the bearing run for 4141 million cycles. b) An SEM image of voids captured within the depth range of LAB where an inclusion was removed during polishing.

To confirm the origin of these features, these cracks have been observed prior to etching on polished surfaces, where similar cracks are seen (compare the images in Figure 9 with those in Figures 6 & 8). This proves conclusive evidence that the voids/micro-cracks are real and not an artefact of the surface preparation (etching). To show this further another sample (4141 million cycles) was optically imaged in an unetched state (Figure 10a), then imaged after etching (Figure 10b), followed by higher resolution SEM imaging of four sites/features showing crackss (Figures 10c-f). Figure 10c and Figure 10d show SEM images of cracks surrounding NMIs while Figure 10e and Figure 10f show cracks developing directly at the weak planes of the LABs discussed in section 3.1. Comparing the position of these cracks in Figure 10a and Figure 10b demonstrates the development of these features in the region where WEBs exist rather than regions without WEB.

It is thus concluded that in the bearing samples, without surface damage, cracks are developed with the WEB region in the subsurface. Cracks are shown to originate from the weak planes of the lenticular carbides and ferrite regions of the WEBs which is more frequent in late LAB stages (dense regions) and the interaction of WEBs with inclusions has also shown to contribute to both micro-cracks and loss of inclusion coherence that may lead to eventual surface spallation. However, since the bearings investigated in this section do not have surface damage or even crack propagation. The next section will focus on a failed bearing test to investigate the links between these cracks and bearing failures.

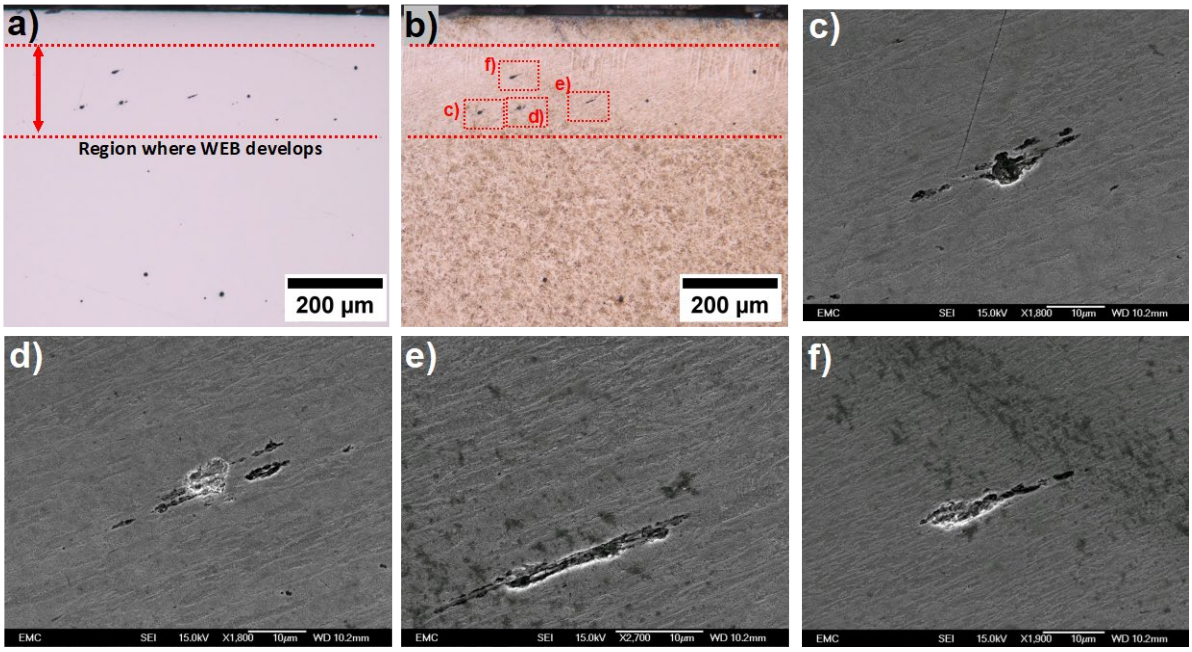

Figure 10: Examination of bearing sample run for 4141 million cycles showing voids developing within the WEB region in a) unetched surface and b) etched surface. c-f) SEM images of voids from etched surface in b).

3.3 WEBs and cracks in failed bearing sample

Figure 11 presents optical and SEM images of a circumference cross-section of an inner ring sample from a bearing with surface spalling failure. Figure 11a shows that the surface spall interacts with the WEBs with a crack running through the bands in the bearing subsurface. Close inspection of the area has shown that the micro-cracks propagating across the WEB region parallel with LABs from the SEM images in Figure 11c-e. The microcracks are observed to align with the interfaces between lenticular carbides (LCs) and the ferrite phases of the LAB as indicated by the white and black arrows respectively. This is similar to the subsurface cracks observed in the undamaged bearing samples above. Again, this suggests there are weak planes in the steel at the interface of between lenticular carbides and equiaxed/elongated ferrite grains contributing to the crack formation, and ultimately final spallation of the bearing. Details on identifying LCs and ferrites can also be found in [24, 35]. While the study of the suspended samples (non-failed) showed evidence of crack initiation at the weak planes of the WEBs, the study of the failed sample shows that crack propagation may occur across LABs, reaching the surface.

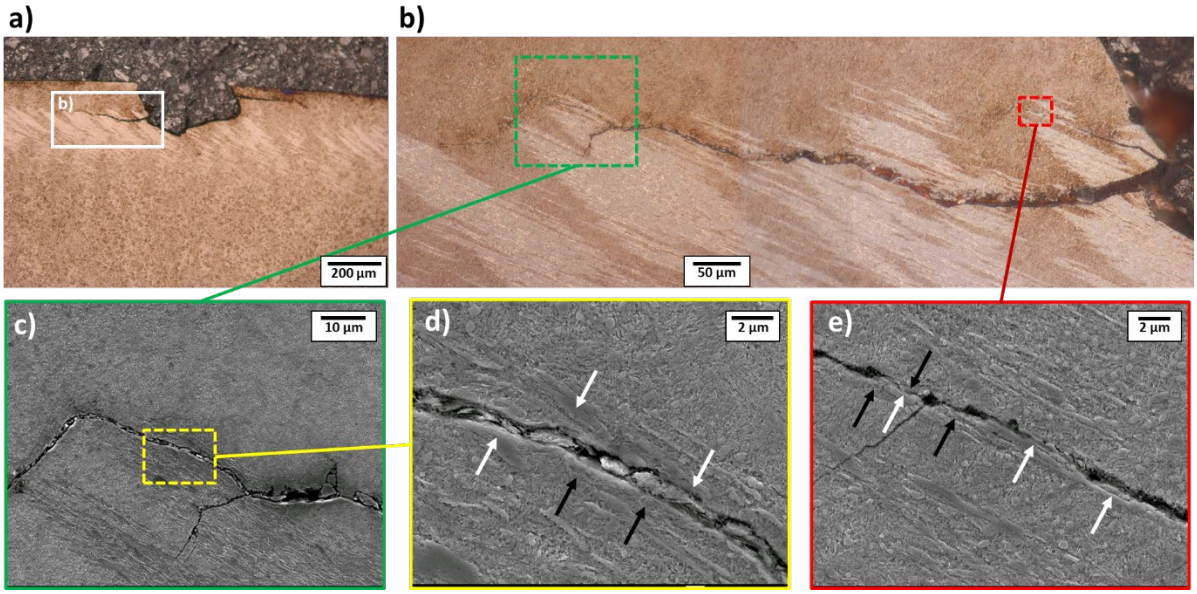

Figure 11: a) Optical Image of spall in failed bearing sample in circumferential cross section. b) Optical image of crack connected to spall bottom and LAB. c) SEM image of microcrack tip showing interaction between crack position and LAB features. d) Enlarged SEM from c) showing crack propagating between ferrite grains and lenticular carbides of LAB. e) SEM image of microcrack parallel to lenticular carbide of LAB. Black arrows indicate ferrite grains in the LAB while white arrows show the lenticular carbides in the LAB.

4. Discussion

The influence of WEBs when they develop in bearings run for very long revolutions on material integrity and spalling has not been well documented in literature prior to this study. An RCF-tested bearing was partially cut through on an axial plane and fractured to induce cracking from the raceway to the bore on an axial plane by Martin et al. [17]. It was reported that the crack proceeded along a straight line normal to the raceway until the crack reached the WEB region, where the crack orientation changed to be like LAB orientations. However, the documentation for this evidence is limited. It has been reported by Voskamp [36] that spalls in bearings without WEB formation have a relatively smooth fractured bottom surface comparing with those with WEBs, which have a rougher bottom surface due to crack propagating across various LABs in the microstructure. This is similar to the findings in this study where the failed sample shows a spall with micro-cracks propagating across LABs and specifically at the interface of ferrite/lenticular carbide. It has been previously reported that the lenticular carbides, equiaxed ferrite grains and elongated ferrite grains in LABs have a hardness of 9.7 GPa, 5 GPa and 4.4 GPa respectively [24]. Regions with higher hardness in the microstructure can act as crack deflectors, especially when surrounded by soft regions (ferrite), making these weak planes become regions susceptible to crack propagation (Figure 11 and initiation (Figure 2-4). The carbide/ferrite interface are known to be preferential sites for dislocation pile-up [37], making it susceptible to the accumulation of stress points and hence, crack formation. However further investigation into the elastic properties at these weak planes could aid in better understanding

how these regions influence crack formation and propagation.

Micro-cracks have been observed in bearings without surface damage tested for stress cycles ranging from 1448 million to 4141 million in this study, while the earliest stage bearing (run for 1116 million cycles) run under 2.9 GPa did not present any voids. This evidence suggests that LABs, especially as they become more developed (denser) at late stages, could promote final bearing failure through both crack propagation and initiation. The commonality of these voids/cracks particularly at late-stage samples (higher operating time) in dense closely packed LAB regions compared to earlier stages LAB [24] suggests these cracks are induced by the microstructural alterations rather than a defect from metallographic preparation. Serial sectioning of these cracks in Figure 4 also supports this statement as they may exceed 12 μm in span across the material while the general span of LAB can extend from 9-102 μm [22]. Throughout the serial sectioning, the cracks are observed to be surrounding the lenticular carbide while the boundary between the lenticular carbides and ferrite grains become more visible as the crack is polished away (see in Figure 4 (slices 8-12)). The damage mechanism of cracks observed across LABs is believed to be correlated with the phase transformation process associated with WEB formation. It has been reported that in dual phase steel, void formation can initiate at interfaces between regions of relatively hard, untempered martensite and relatively soft bainitic ferrite under RCF [38] and later propagate across the softer phase. In comparison, the voids/cracks in this study have been develop between the relatively soft ferrite grains and relatively hard lenticular carbides, while the width of these cracks appear to develop across the ferrite grain as evidenced in Figure 4 as they are gradually removed in serial sectioning.

In literature, inclusions have been investigated corresponding to the microstructural alteration known as butterflies, which consists of wings of WEAs growing from inclusions and white etching cracks [3, 8]. In butterflies, inclusions are considered to be an initiator for their formation due to elastic modulus differences, differing coefficients of thermal expansion and the weak interfacial energy between the inclusion and matrix generating tensile and shear stresses in the locally surrounding matrix. While no link between WEB initiation and inclusions is observed in this study, similar to previous findings [22]. Fully developed WEBs have been observed to propagate across pre-existing inclusions and lead to loss of coherence between the inclusion and surrounding matrix. Evidence from Figure 6a also demonstrates that internal cracks may develop within inclusions at similar orientations to the WEBs penetrating them. While WEB development and growth has been linked to preferential slip systems aligned at 30° and 80° in LABs and HABs respectively [24, 35], this suggests the orientated slip systems extends across to the inclusions if embedded within the WEBs. The development of micro-cracks and loss of coherency of inclusions hence become likely initiation sites for bearing failure. This has been observed in

both Alumina and MnS inclusions which are the most common types in bearing steels (Figure 6a,c).

The crack formation at edges of inclusions (see Figure 7) is similar to that observed in butterflies. These observations are typically observed at hard inclusions under rolling conditions where cavities develop at the interfaces due to de-bonding of the two parts [1, 28]. This suggests that the inclusions removed in Figure 7 are likely to have been hard inclusions such as alumina. Nonetheless, it is frequently observed that cavities form and inclusions lose their coherence in the region of WEBs compared to areas without WEB formation, as evidenced in Figure 6 -10. The deformation of these inclusions is more pronounced when surrounded by WEBs which is likely due to the volume reduction associated with the microstructural transformation of martensite to ferrite, hence tensile stress build-up in the region could be a factor enhancing the deformation of inclusions compared to inclusions surrounded by the parent matrix as mentioned previously. FE modelling of MnS inclusions under RCF has shown stress concentrations accumulating at the edges of the inclusions in a similar geometry to that observed in butterfly wings [39]. It is also shown that loss of coherence between inclusion and surrounding matrix can lead to an increase of stress concentration of up to 167% at the edges. The cavity formation around inclusions is also heavily dependent on the relative hardness difference between the inclusion and surrounding matrix [40]. Hence, multiple factors appear to contribute to the observed phenomena in this study to explain both the debonding of inclusions surrounded by WEBs, and the propagation of voids/micro-crack from the inclusion/matrix interface towards the carbide/ferrite boundary in the WEBs.

It is interesting to compare the inclusion damages (coherence loss, internal cracks in inclusion and cracks across the steel matrix) caused by WEBs in this study and butterflies which are commonly reported. As previously mentioned, all inclusion interactions with the WEBs in this study is from inclusions with a diameter below 10 μm, which is smaller than those typically associated with butterflies where inclusion diameters of over 20 μm have been typically reported [32, 41]. Given that some inclusions are observed to have been removed during polishing (Figures 8 and 9), it is suggested that these inclusions have experienced significant debonding compared to other microstructural alterations associated with inclusions such as butterflies. However, no crack network is seen to have developed across the material as in butterflies. Also, micro-cracks appear to grow across the weak planes of the pre-existing LABs whereas butterflies show cracks across the material with newly developed nanocrystalline white etching areas surrounding them [1, 3, 6].

The two main contributors to subsurface void/crack formation in bearing steels in this scenario (running for very high number of revolutions) that can affect the integrity of rolling element bearings is thus summarized in Figure 12, showing how WEBs can contribute to bearing failures through, either a) dislocation pile-up at the

carbide/ferrite interface, leading to void/crack formation at these weak planes, or b) WEB growth through or around non-metallic inclusions leading to de-bonding of NMIs from the steel matrix as well as micro-crack formation within inclusions. The majority of cracks observed in this study are related to the NMI/WEB interaction which suggests inclusions are the likely initiation sites for these micro-cracks while the penetrating WEBs provide weak planes to cause the propagation of these damages from the inclusions.

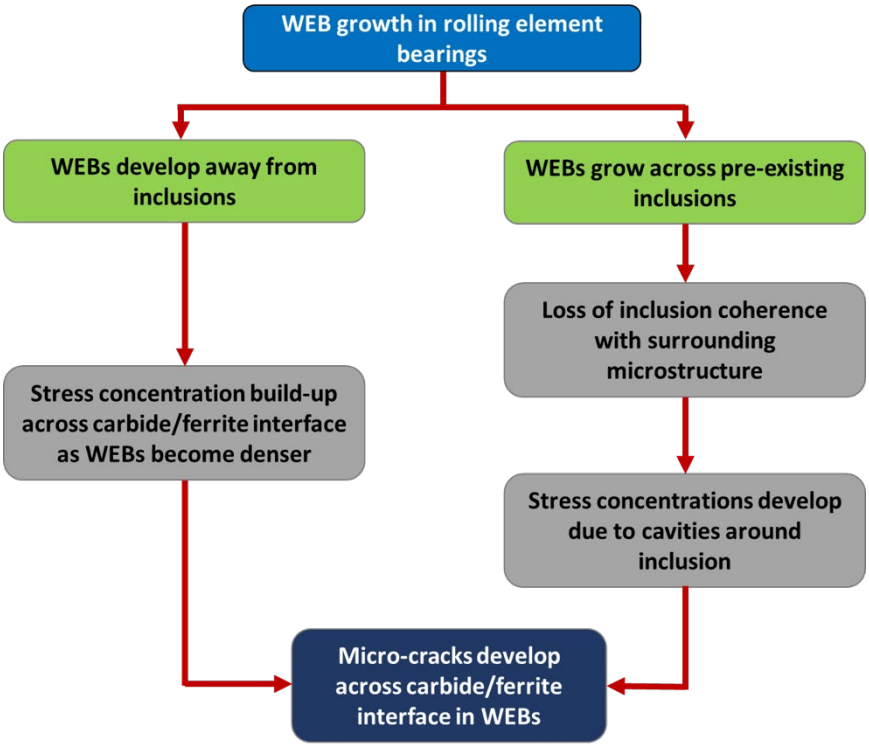

Figure 12: A flow chart illustrating the two routes that WEBs contribute to micro-crack development in rolling bearing steel.

5. Conclusion

This study has focused on analyzing the influence of WEBs (including LABs and HABs) on the integrity of steel bearings under RCF. A number of tested bearing inner rings at different fatigue stages have been analysed with and without surface spallation. Conclusions from this study are summarized below:

- Crack networks branching from the surface spall in a failed bearing sample has shown to propagate across LABs in its proximity and aligned with the interface between lenticular carbides and the ferrite grains in the LABs that is considered as a plane of weakness in the microstructure where the carbides act like as crack deflectors.
- The crack networks leading to the final spall are potentially linked to voids and micro-cracks formed in WEBs at earlier stages of the RCF in suspended bearings. Formation of voids in the subsurface of bearing samples with no spall is observed at the interface of lenticular carbides and ferrite grains of late-stage

LABs. It is more frequent in regions with dense closely packed LABs compared to sparse LABs. The voids/micro-cracks observed vary in width from 500 nm to 2 µm, the lengths recorded vary from 1 µm to over 10 µm while serial sectioning has shown that the span of the cracks can exceed 12 µm.

- Although the contribution of WEBs to bearing spalling may be minor, WEBs (both LAB and HAB) growing through inclusions result in loss of coherence of the inclusions from their surrounding matrix consisting of WEBs. This leads to cavity formation around the inclusion and cracks developing at the edge of the inclusions and growing through the weak planes (carbide/ferrite interface) of LABs.

Experimental evidence of LABs and HABs contributing to fatigue spalling has been given in this study through detailed analysis, showing the development of cracks in the subsurface within the WEBs and through interacting with surrounding inclusions. It has also been shown that WEBs can influence crack propagation in failed samples and can even cause crack initiation in bearings that have not failed. This manuscript has provided new evidence in the fundamental understanding of microstructural behavior during the RCF process in bearings and its influence on the material integrity in bearings operating for very high number of revolutions.

6. Acknowledgements

This research has been co-funded by ESPRC (EP/N509747/1) and Schaeffler Technologies AG & Co. KG, Schweinfurt, Germany.

References

[1] M. El Laithy, L. Wang, T. J. Harvey, B. Vierneusel, M. Correns and T. Blass, "Further understanding of rolling contact fatigue in rolling element bearings-a review," *Tribology International,* p. 105849, 2019.

[2] F. Sadeghi, B. Jalalahmadi, T. S. Slack, N. Raje and N. K. Arakere, "A review of rolling contact fatigue," *Journal of tribology,* vol. 131, p. 041403, 2009.

[3] M. Evans, "An updated review: white etching cracks (WECs) and axial cracks in wind turbine gearbox bearings," *Materials Science and Technology,* vol. 32, no. 11, 2016.

[4] Q. Lian, . G. Deng, H. Zhu, H. Li, X. Wang and Z. Liu , "Influence of white etching layer on rolling contact behavior at wheel-rail interface," *Friction,* vol. 8, pp. 1178-1196, 2020.

[5] V. Šmeļova, A. Schwedt, L. Wang, W. Holweger and J. Mayer, "Microstructural changes in white etching cracks (WECs) and their relationship with those in dark etching region (DER) and white

etching bands (WEBs) due to rolling contact fatigue (RCF)," *International Journal of Fatigue,* vol. 100, pp. 148-158, 2017.

[6] F. Lopez-Urunuela, B. Fernandez-Diaz, F. Pagano, A. Lopez-Ortega, B. Pinedo, R. Bayon and J. Aguirrebeitia, "Broad review of “White Etching Crack” failure in wind turbine gearbox," *International Journal of Fatigue,* vol. 145, p. 106091, 2021.

[7] A. Grabulov, U. Ziese and H. Zandbergen, "TEM/SEM investigation of microstructural changes within the white etching area under rolling contact fatigue and 3-D crack reconstruction by focused ion beam," *Scripta Materialia,* pp. 635-638, 2007.

[8] H. Bhadeshia and W. Solano-Alvarez, "Critical Assessment 13: Elimination of white etching matter in bearing steels," *Materials Science and Technology,* vol. 31, no. 9, 2015.

[9] A. Ruellan, X. Kleber and F. Ville, "Understanding white etching cracks in rolling element bearings: Formation mechanisms and influent tribochemical drivers," *Journal of Engineering Tribolgy,* vol. 229, no. 8, 2015.

[10] R. Tricot, J. Monnot and M. Lluansi, "How microstructural alterations effect fatigue properties of 52100 steel," *Metals engineering quarterly,* vol. 12, pp. 39-47, 1972.

[11] R. Hyde, "Microstructural changes from contact fatigue," in *ASM Handbook - Vol 19 Fatigue andf Fracture*, 1996, pp. 1749-1780.

[12] R. Osterlund, O. Vingsbo, L. Vincent and P. Guiraldenq, "Butterflies in fatigued ball bearings - formation mechanism and structure," *Scandinavian Journal of Metallurgy,* pp. 23-32, 1982.

[13] A. Vincent, G. Lormand, P. Lamagnère, L. Gosset, D. Girodin, G. Dudragne and R. Fougères, "From white etching areas formed around inclusions to crack nucleation in bearing steels under rolling contact fatigue," in *J.J.C. Hoo, W.B. Green (Eds.) Bearing Steels: Into the 21st Century*, West Conshohocken, ASTM, 1998, pp. 109-123.

[14] K. Böhm, H. Schlicht, O. Zwirlein and R. Eberhard, "Nonmetallic inclusions and rolling contact fatigue, Bearing Steels: The Rating of Nonmetallic Inclusions,," Boston, ASTM, 1974, pp. 96-113.

[15] H. Schlicht, E. Schreiber and O. Zwirlein, "Effects of material properties on bearing steel fatigue strength, in: J.J.C. Hoo (Ed.) Effect of steel manufacturing processes on the quality of bearing steels," Philadelphia, ASTM, 1988, pp. 81-101.

[16] N. Maharjan, W. Zhou and Y. Zhou, "Micro-structural study of bearing material failure due to rolling contact fatigue in wind turbine gearbox," in *Proceedings of the international symposium on current research in hydraulic turbines, Kathmandu University, Dhulikhel, Nepal*, 2016.

[17] J. A. Martin, S. F. Borgese and A. D. Eberhardt, "Microstructural alterations of rolling—bearing steel undergoing cyclic stressing," *Journal of Basic Engineering,* vol. 88, pp. 555-565, 1966.

[18] N. H. Forster, L. Rosado, W. P. Ogden and H. K. Trivedi, "Rolling contact fatigue life and spall propagation characteristics of AISI M50, M50 NiL, and AISI 52100, Part III: metallurgical examination," *Tribology Transactions,* vol. 53, pp. 52-59, 2009.

[19] H. Swahn, P. Becker and O. Vingsbo, "Martensite decay during rolling contact fatigue in ball bearings," *Metallurgical transactions A,* vol. 7, pp. 1099-1110, 1976.

[20] A. Warhadpande, F. Sadeghi and R. D. Evans, "Microstructural alterations in bearing steels under rolling contact fatigue Part 1—Historical overview," *Tribology Transactions,* vol. 56, pp. 349-

358, 2013.

[21] M. El Laithy, L. Wang, T. Harvey, A. Schwedt, B. Vierneusel and J. Mayer, "Mechanistic study of dark etching regions in bearing steels due to rolling contact fatigue," *Acta Materialia,* vol. 246, p. 118698, 2023.

[22] M. El Laithy, L. Wang, T. Harvey and B. Vierneusel, "Re-investigation of dark etching regions and white etching bands in SAE 52100 bearing steel due to rolling contact fatigue," *International Journal of Fatigue,* vol. 136, p. 105591, 2020.

[23] M. El Laithy, L. Wang, T. Harvey and B. Vierneusel, "Semi-empirical model for predicting LAB and HAB formation in bearing steels," *International Journal of Fatigue,* vol. 148, p. 106230, 2021.

[24] M. El Laithy, L. Wang, H. Terry, A. Schwedt, B. Vierneusel and J. Mayer, "White etching bands formation mechanisms due to rolling contact fatigue," *Acta Materialia,* p. 117932, 2022.

[25] H. Fu and P. E. J. Rivera-Díaz-del-Castillo, "Evolution of White Etching Bands in 100Cr6 Bearing Steel under Rolling Contact-Fatigue," *Metals,* vol. 9, p. 491, 2019.

[26] F. Ebert, "Fundamentals of design and technology of rolling element bearings," *Chinese Journal of Aeronautics,* vol. 23, no. 1, pp. 123-136, 2010.

[27] S. Li, "Effects of inclusions on very high cycle fatigue properties of high strength steels," *International Materials Reviews,* vol. 57, no. 2, pp. 92-114, 2012.

[28] P. Walker, "Improving the reliability of highly loaded rolling bearings: the effect of upstream processing on inclusions," *Materials Science and Technology,* vol. 30, no. 4, pp. 385-410, 2014.

[29] J. Lankford, "“(e) effect of oxide inclusions on fatigue failure,," *International Metals Reviews,* vol. 22, no. 1, pp. 221-228, 1977.

[30] M. Dinkel and W. Trojahn, "Influence of sulfur inclusion content on rolling contact fatigue life," in *Bearing Steel Technologies: 10th Volume, Advances in Steel Technologies for Rolling Bearings*, ASTM International, 2014.

[31] Schaeffler Technologies, "Load carrying capacity and rating life," in *Lubrication of Rolling Bearings*, 2013, pp. 14-24.

[32] M. Evans, A. Richardson, L. Wang and R. Wood, "Serial sectioning investigation of butterfly and white etching crack (WECs) formation in wind turbine gearbox bearings," *Wear,* vol. 302, 2013.

[33] A. P. Voskamp, R. Österlund, P. C. Becker and O. Vingsbo, "Gradual changes in residual stress and microstructure during contact fatigue in ball bearings," *Metals Technology,* vol. 7, pp. 14-21, 1980.

[34] T. Waterschoot, K. Verbeken and B. De Cooman, "Tempering Kinetics of the Martensitic Phase in DP Steel," *ISIJ international,* vol. 46, pp. 138-146, 2006.

[35] V. Šmeļova, A. Schwedt, L. Wang, W. Holweger and J. Mayer, "Electron microscopy investigations of microstructural alterations due to classical Rolling Contact Fatigue (RCF) in martensitic AISI 52100 bearing steel," *International Journal of Fatigue,* vol. 98, pp. 142-154, 2017.

[36] A.Voskamp, "Material Response to rolling contact loading," *J Tribol,* vol. 107, pp. 359-364, 1985.

[37] J. Languillaume, G. Kapelski and B. Baudelet, "Cementite dissolution in heavily cold drawn pearlitic steel wires," *Acta Materiala,* vol. 45, no. 3, pp. 1201-1212, 1997.

[38] W. Solano-Alvarez, E. Pickering and H. Bhadeshia, "Degradation of nanostructured bainitic steel under rolling contact fatigue," *Materials Science and Engineering: A,* vol. 617, pp. 156-164, 2014.

[39] H. A. Al-Tameemi and H. Long, "Finite element simluation of subsurface intiated damage from non-metallic inclusions in wind turbine gearbox bearings," *International Journal of Fatigue,* vol. 131, p. 105347, 2020.

[40] S. Deng, L. Hua, X. Han and S. Huang, "Investigation of rolling contact fatigue cracks in ball bearings," *International Journal of Fracture,* vol. 188, pp. 71-78, 2014.

[41] M. Evans, "White structure flaking (WSF) in wind turbinegearbox bearings: effects of ‘butterflies’ andwhite etching cracks (WECs)," *Materials Science and Technology,* vol. 28, pp. 3-22, 2012.